Effects of external stress field on the charge stability of nitrogen vacancy centers in diamond

Miao-Miao Yao, Tian-Yuan Zhu, and Da-Jun Shu[a)]
National Laboratory of Solid State Microstructures, School of Physics, and Collaborative Innovation Center of Advanced Microstructures, Nanjing University, Nanjing 210093, China

(Received 7 April 2017; accepted 20 July 2017; published online 28 July 2017)

The interaction of the atom-like defects in semiconductors with external fields provides an avenue to quantum information processing and nanoscale sensors. Meanwhile, external fields may induce instability of the desired charge state of the defects. It is essential to understand how the charge state of a defect is affected by external fields that introduced in diverse applications. In this letter, we explore the stability of the negatively charged state (NV^-) and the neutral state (NV^0) of the nitrogen vacancy (NV) center in diamond under stress by first-principles calculations. We find that the relative stability of NV^- to NV^0 is always reduced by the stress if the NV center is free to relax its orientation. Once the NV center has formed and retains its orientation, however, the relative stability of NV^- can be always enhanced by compressive stress along its trigonal symmetry axis. We believe that the results are not only significant for control of the charge stability of NV center but also enlightening for applications based on specific charge states of other kinds of defects in the stress field. *Published by AIP Publishing.* [http://dx.doi.org/10.1063/1.4997025]

Atom-like defects in semiconductors possess unique properties that make them attractive for solid-state electronics.[1] Due to the difference in the localized electronic structures of the defects in different charge states, practical applications usually require a defect to be stable in a specific charge state. On the other hand, instability of the charge state of a defect may be induced by the external fields introduced in applications.[2] Because stochastic transitions between different charge states are detrimental to the efficiency of the defect-related applications, it is essential to understand how the charge state of a defect is affected by different kinds of external fields that are introduced in diverse applications.

As a prototype of an atom-like system, the nitrogen vacancy (NV) center in diamond is one of the most promising candidates for solid-state quantum information processing and nano-sensors in physics and biology.[3–11] The NV center primarily appears in the negative charged state (NV^-) or in the neutral state (NV^0), with quite different optical and magnetic properties.[12] Among them, most of the spin-related applications are based on the properties of NV^-. The charge state of an NV center in equilibrium can be manipulated by temperature, defects, surface chemistry, and gate electrode, mediated by the change in the defect level relative to the Fermi energy.[13–16] Besides, the NV center can be ionized by the external field, which drives the distribution of different charge states away from equilibrium.[17] Transitions between different charge states of nitrogen vacancy center in diamond are reported to be induced by laser illumination and electric fields.[18–21]

Apart from the optical and electrical fields, the stress field is unavoidable in many practical applications. It includes the accumulated stress during the non-equilibrium growth process, the stress due to the lattice mismatch, and the mechanically generated stress.[22–28] Influences of external stress on formation, distribution, and diffusivity of defects in semicondutors have been reported previously.[29–31] For the nitrogen vacancy (NV) center in diamond, it has been predicted that the NV orientation can be controlled by the external stress.[32] Experimentally, coupling between the stress field and the spin of the NV center makes it possible to measure the pressure or stress tensor, to drive magnetically forbidden spin transition, to mediate the long-range spin-spin interaction, and so on.[11,28,33–36] Anisotropic stress and hydrostatic pressure ranging from 100 MPa to 60 GPa have been introduced in the experiments. However, it remains unclear about the influence of stress on the charge state of the NV center in diamond.

In this letter, we investigate the relative stability of NV^- to NV^0 in diamond under homogeneous external stress by using first-principles calculations. We find that anisotropic external stress is harmful for the relative stability of NV^- to NV^0 if the NV center is free to relax its orientation. Once the orientation of an NV is frozen after formation, however, compressive stress along its trigonal symmetry axis is always beneficial to the relative stability of NV^-. Besides, uniaxial tensile stress along [111] or biaxial compressive stress within the (111) plane can also improve the relative stability of NV^- to NV^0 if the stress breaks the C_{3v} symmetry of NV^- while maintaining the stable configuration of NV^0. The uncovered effect of the stress field on the charge stability of the NV center would be of general essence for applications based on the specific charge state of defects in solids.

The calculations are based on the density functional theory in the PBE generalized gradient approximation (GGA), using the Vienna *ab initio* simulation package (VASP) with projector augmented wave pseudo-potentials.[37] Although the GGA functional is known to underestimate the energy gap of semiconductors and thus the defect levels, it is reliable to obtain their changing trend under external stress. The plane-wave cutoff is set as large as 840 eV in order to obtain

[a)]djshu@nju.edu.cn

convergent elastic properties. The lattice constant of diamond is calculated to be 3.573 Å with the sampled Brillouin zone of the primitive cell using a $12 \times 12 \times 12$ Monkhorst-Pack k-point mesh,[38] close to the experimental value of $a_0 = 3.567$ Å. A cubic $(3 \times 3 \times 3)$ supercell is used to model the bulk diamond in which an NV center is introduced, using a $4 \times 4 \times 4$ Monkhorst-Pack k-point mesh. External stress within ±40 GPa is applied in three different ways. One is the isotropic stress σ_{hyd}, which if compressed corresponds to the hydrostatic pressure. The other two types of anisotropic stress are applied biaxially within the (111) plane and along the [111] direction, denoted hereafter as $\sigma_{(111)}$ and $\sigma_{[111]}$, respectively. We first calculate the elastic constants for the non-defective diamond, which are 1051 GPa, 126 GPa, and 563 GPa for C_{11}, C_{12}, and C_{44}, respectively. The elastic modulus and Possion coefficients are obtained under different external stress conditions, in consistent with previous reports.[39,40] Assume that the elastic properties are influenced little by the defects of low-density, and the elastic properties of the non-defective diamond are used to determine the strain tensor of NV-contained diamond under different external stress according to the elastic theory.

Under zero stress, the NV^- centers are C_{3v} symmetric with their trigonal symmetry axis along the NV orientation in the ⟨111⟩ direction. In contrast, the symmetry of NV^0 after relaxation is reduced to C_{1h} due to the Jahn-Teller effect.[41] We find that the N atom can move either toward one of the three neighboring carbon atoms (C_3) or toward the center of the two equivalent carbon atoms (C_{12}). The corresponding configurations are hereafter denoted as s_1 and s_2, respectively. In s_1, the bond length of NC_{12} is larger than that of NC_3, and the opposite is in s_2, as shown in Fig. 1. Configuration s_1 is energetically more stable than s_2 by about 0.07 eV under zero stress.

The NV centers under stress are categorized into two different types depending on whether the C_{3v} symmetry of NV^- remains or is broken. Isotropic stress σ_{hyd} does not break the symmetry, so all the NV centers fall into type A. Under $\sigma_{(111)}$ or $\sigma_{[111]}$, however, only NV centers oriented along the [111] direction are of type A. The NV centers oriented along $[1\bar{1}\bar{1}]$, $[\bar{1}1\bar{1}]$, and $[\bar{1}\bar{1}1]$ directions belong to type B because their symmetries are broken by $\sigma_{(111)}$ and $\sigma_{[111]}$.

The N-C bond lengths in A-type and B-type NV centers under external stress are shown in Figs. 2 and 3, respectively. A common feature is that all the bond lengths vary in a linear way with stress. The slopes of the three NC bond lengths in A-type NV with stress are approximately the same as each other and are independent of the charge state of the NV center. Therefore, the bond lengths of NC_{12} are always larger (smaller) than those of NC_3 in configuration s_1 (s_2) of NV^0. For clarity, only bond lengths in s_1 are shown in Fig. 2. We can see that the bond lengths increase with σ_{hyd} and $\sigma_{(111)}$, while decrease with $\sigma_{[111]}$ to a lesser degree.

For B-type NV under external stress, as the symmetry of NV^- is broken, the three NC bonds in NV^- fall into two inequivalent ones, denoted, respectively, also as NC_{12} and NC_3. The NC bond lengths in both NV^0 and NV^- increase with both $\sigma_{(111)}$ and $\sigma_{[111]}$. Moreover, NC_{12} is *softer* than NC_3 under $\sigma_{(111)}$ and conversely under $\sigma_{[111]}$. It is reasonable because NC_3 bond of the B-type NV center prefers to be along the [111] direction under $\sigma_{(111)}$ and $\sigma_{[111]}$. As a result, the length of NC_3 in configuration s_1 of NV^0 becomes larger than that of NC_{12} when compressive $\sigma_{(111)}$ or tensile $\sigma_{[111]}$ is around 10 GPa, as shown in Figs. 3(a) and 3(d). The different responses of the NC bonds are expected to play a key role in the relative stability of NV^0 in s_1 and s_2 configurations under anisotropic stress, as will be discussed below.

The formation energy of the NV center in charge state q is calculated by the following equation:[42,43]

$$E^f[NV^q] = E_{tot}[NV^q] - E_{tot}[bulk] + E^q_{corr} - \mu_N + 2\mu_C + q\left[\epsilon_\nu + \epsilon_F + \triangle v_{0|b}\right], \quad (1)$$

where $E_{tot}[NV^q]$ is the total energy of the supercell with defect NV in charge state q and $E_{tot}[bulk]$ is the total energy of the non-defective bulk supercell. The chemical potentials μ_N and μ_C are defined to be one half of the energy of the N_2 molecule and the energy per atom of bulk diamond, respectively. E^q_{corr} accounts for the finite-size supercell corrections, including the spurious Coulomb interaction between charged defects and the nonphysical dispersion of the defect states introduced by use of the supercell model.[44–49] The fermi level ϵ_F is referenced to the valence band maximum ϵ_ν in the nondefective bulk supercell. The last term within the brackets is $\triangle v_{0|b} = v_{0|far} - v_b$, the difference of the electrostatic potential of a reference atom away from the defect, which is used to align ϵ_F of the defective supercell and the non-defective one.

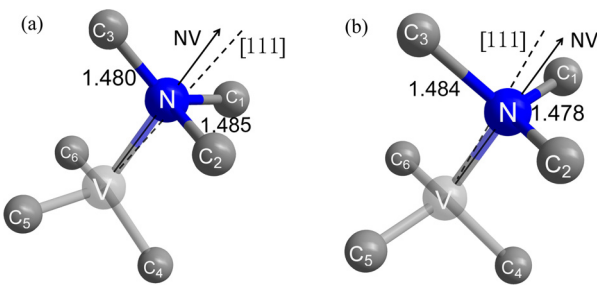

FIG. 1. Schematic show of the structures of an NV^0 orientated along [111] direction under zero-stress, in (a) configuration s_1 and (b) configuration s_2. The bond lengths are in unit of angstrom. The dashed line marks the [111] direction, and the solid arrow shows the orientation of the NV center. Note that the deviation of the NV orientation off the [111] direction is enlarged for clarity.

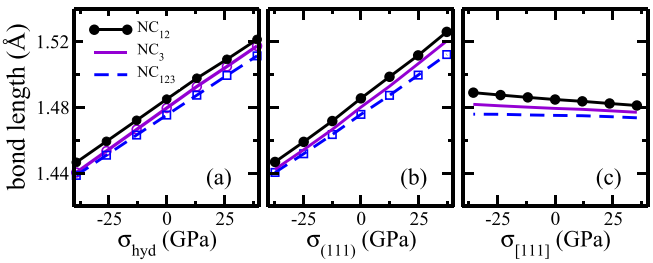

FIG. 2. Variation of the N-C bond distances of A-type NV center under (a) hydrostatic stress, (b) biaxial stress, and (c) uniaxial stress. Solid lines show the N-C bond distance for NV^0 in configuration s_1, with NC_{12} denoting the bond distance between N and the two equivalent C_1 and C_2, and NC_3 the bond distance between N and the third carbon atom C_3. Dashed lines (NC_{123}) show the bond distance between N and the three equivalent C atoms in NV^-.

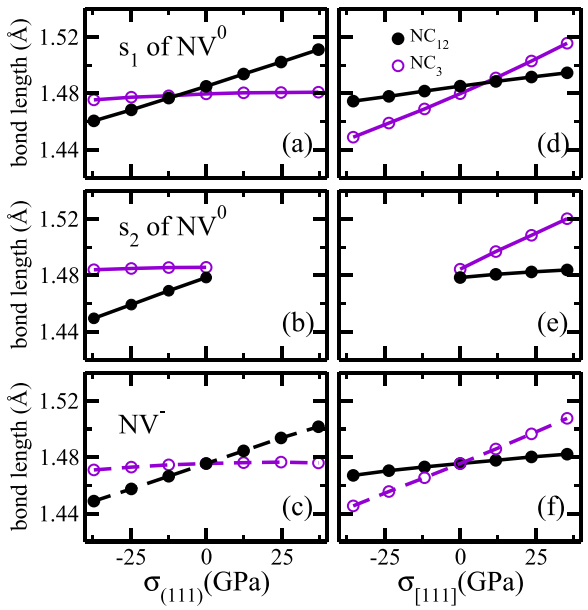

FIG. 3. The N-C bond distances in B-type NV center as a function of stress. The stress is applied within the (111) plane (left) or along the [111] direction (right). The first two rows correspond to configurations s_1 and s_2 of NV^0, and the bottom row is for the NV^-.

The defect levels of NV in a $(3 \times 3 \times 3)$ supercell are approximately flat as previously reported.[50] Therefore, the dispersion correction is negligible. To check the convergence of electrostatic interactions in the supercell model, we calculate the formation energies of the NV^- additionally using a $(2 \times 2 \times 2)$ supercell with a $6 \times 6 \times 6$ Monkhorst-Pack k-point mesh. The difference of $E^f[NV^-]$ between $(2 \times 2 \times 2)$ and $(3 \times 3 \times 3)$ supercell is –0.06 eV under zero stress. Corrections according to the Makov-Payne scheme[44] shift the difference up to 0.11 eV, which obviously overcorrects the electrostatic interaction of charged defects. Fortunately, the corrections of the absolute values of the formation energies are not important here since we mainly focus on the variation of the formation energies under stress. To avoid any factitious errors, we hereafter simply throw off the term E^q_{corr} as adopted in the previous work.[51]

The formation energy of the NV center varies with stress depending on the type of the stress. First, we find that $E^f[NV^0]$ of A-type NV^0 in either s_1 or s_2 configuration changes monotonically in a similar way, increasing with $\sigma_{(111)}$ while decreasing with $\sigma_{[111]}$. Therefore, s_1 is always more stable than s_2. For clarity, we only show the formation energy of s_1 in Fig. 4. In contrast, $E^f[NV^0]$ of the B-type NV^0 in s_1 and s_2 changes with stress in opposite trends. As shown in Figs. 4(d) and 4(g), configuration s_2 becomes more favorable than s_1 under $\sigma_{(111)}$ smaller than –8.66 GPa or under $\sigma_{[111]}$ larger than 11.79 GPa. From the middle row of Fig. 3, it is evident that the stable configuration transits from s_1 to s_2 when the bond length of NC_{12} in s_1 becomes smaller than that of NC_3. Along with the transition, the formation energy of B-type NV^0 reaches its maximum. We would like to point out that in previous reports, only s_1 is identified as the stable configuration.[13] According to our results, however, it is clear that either s_1 or s_2 can be stable under different stresses.

As shown in Fig. 4, $E^f[NV^0]$ decreases under hydrostatic stress, no matter the stress is tensile or compressive. Under anisotropic stress, the variation of $E^f[NV^0]$ under external stress shows different trends for different NV types. A-type NV^0 becomes energetically more favorable under compressive $\sigma_{(111)}$ and tensile $\sigma_{[111]}$. Instead, B-type NV^0 is more favorable under tensile $\sigma_{(111)}$ and compressive $\sigma_{[111]}$. This is consistent with a previous report.[32] The formation energy of NV^- under stress roughly varies in a similar trend of that of NV^0 but to a lesser degree, as can be seen in the middle row of Fig. 4. Similarly, A-type NV^- is energetically more favorable under compressive $\sigma_{(111)}$ and tensile $\sigma_{[111]}$, while B-type NV^- is more favorable under tensile $\sigma_{(111)}$ and compressive $\sigma_{[111]}$.

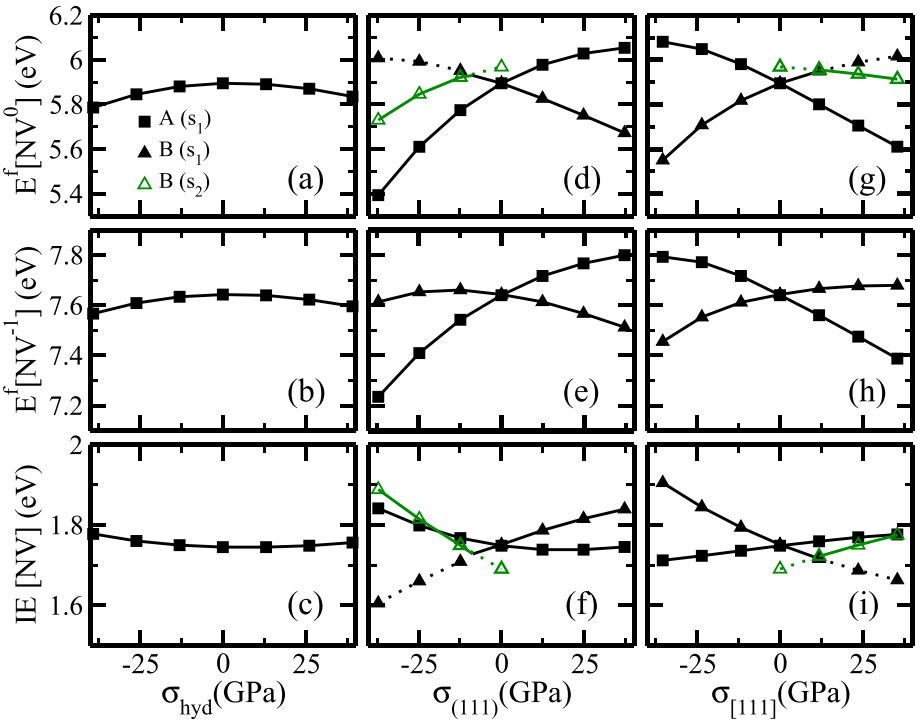

FIG. 4. Formation energy of NV^0 (upper), $NV^-(E_f = 0)$ (middle), and the ionization energy (bottom) as functions of hydrostatic stress (a)–(c), biaxial stress (d)–(f), and uniaxial stress (g)–(i). Squares and triangles represent A-type and B-type NV centers, respectively. Configuration s_1 and s_2 of NV^0 are denoted by solid and open symbols, respectively. For A-type NV^0, we only show the formation energies of configuration s_1 because s_1 is always more stable than s_2.

Considering the different sign of the strain along the [111] direction caused by $\sigma_{(111)}$ and $\sigma_{[111]}$, it suggests that the NV center prefers to align with its symmetry axis along the tensile direction while off the compressive direction. If the NV center is free to relax its orientation, the formation of the NV center always becomes easier under stress than under the zero-stress condition. In this sense, external stress in the formation process would promote the formation of NV centers.

The relative stability of NV^- to NV^0 can be described by the difference of their formation energies. Combined with Eq. (1), it follows that $\Delta E^f = (E^f[NV^-]_{\epsilon_F=0} - E^f[NV^0]) - \epsilon_F$. There exists a critical fermi level above which ΔE^f becomes negative, and NV^- is more stable than NV^0. It corresponds to the $(0/-)$ charge transition level, also referenced as the ionization energy (IE) of the NV center.[45,52] Obviously, the ionization energy is equal to the difference ΔE^f at the zero fermi level

$$IE[NV] = E^f[NV^-]_{\epsilon_F=0} - E^f[NV^0]. \quad (2)$$

A smaller IE means a lower ϵ_F above which NV^- is more stable than NV^0. Therefore, it corresponds to higher relative stability of NV^- against transforming into NV^0.

The ionization energy is calculated and shown in the bottom row of Fig. 4. By comparing the first two rows with the third one in Fig. 4, one can see that the ionization energy changes with the stress in an opposite trend of the formation energy, which can lead to some unexpected conclusions. First, while compressive $\sigma_{(111)}$ and tensile $\sigma_{[111]}$ are beneficial to the formation of A-type NV, they reduce the relative stability of NV^- to NV^0. Similarly, under tensile $\sigma_{(111)}$ or compressive $\sigma_{[111]}$, B-type NV is more favorable, but the relative stability of the B-type NV^- to NV^- is reduced. Therefore, if an NV center is free to relax its orientation during the fabrication process, the stress is always harmful for the relative stability of NV^- to its neutral state. Second, if the orientation of an NV center is frozen after its formation, external stress may reduce or enhance the relative stability of NV^-. According to the bottom row of Fig. 4, continuous decrease of the ionization energy occurs for A-type NV under compressive $\sigma_{[111]}$. It indicates that if the NV center has already formed and remains in its orientation, the relative stability of an NV^- against transforming into an NV^0 can be improved by applying compressive stress along the symmetry axis of the NV center.

In order to connect with the experiments, we make an estimation of lifetime ratio between NV^- and NV^0. It follows that $R(\sigma) = R(0)\exp(-[IE(\sigma) - IE(0)]/k_BT)$, where $R(0)$ and $R(\sigma)$ are the lifetime ratios under the zero-stress condition and external stress, respectively, k_B is the Boltzmann constant, and T is the concerned temperature. At room temperature, stress within 2.0 GPa does not induce obvious change in the lifetime ratio. However, $R(\sigma)$ under larger stress changes obviously depending on the type of the stress. For instance, compressive $\sigma_{[111]}$ of 40 GPa increases the lifetime ratio $R(\sigma)$ of A-type NV by about 5 times, while the same stress level applied in other directions reduces $R(\sigma)$. For B-type NV, $R(\sigma)$ increases with compressive $\sigma_{(111)}$ and tensile $\sigma_{[111]}$ if the stress is not large enough to transit the stable configuration of NV^0 from s_1 to s_2. Therefore, $R(\sigma)/R(0)$ of B-type NV reaches its maxima along with the transition when $\sigma_{(111)} = -8.66$ GPa and $\sigma_{[111]} = 11.79$ GPa, which are about 2.2 and 4.0, respectively. The effect becomes more dramatic at cryogenic temperature. $R(\sigma)$ of A-type NV increases by about 4 times and 540 times under compressive $\sigma_{[111]}$ of 10 GPa and 40 GPa, respectively. The maximal $R(\sigma)/R(0)$ of B-type NV is about 20 or 215 at cryogenic temperature, under compressive $\sigma_{(111)}$ and tensile $\sigma_{[111]}$ GPa, respectively.

In summary, the stress is found to have an important influence on the charge stability of nitrogen vacancy center in diamond. Although it favors the formation of the NV center, the externally applied stress is harmful for the relative stability of NV^- to its neutral state if the NV center is free to relax its orientation during the fabrication process. Once the NV center has formed and the orientation is frozen, however, compressive stress along the NV orientation is always beneficial to the stability of NV^- against the less viable NV^0. The predictions are significant for applications based on NV^- centers in diamond, especially for those utilizing the coupling between the stress field and the spin of the NV center. Furthermore, the uncovered important influence of the stress field on the charge stability of defects would be of general essence for applications based on the specific charge state of defects in solids.

The numerical calculations have been carried out at the National Supercomputer Center in Tianjin. This work was supported by the National Natural Science Foundation of China (Grants No. 11174123) and the Basic Research Program of Jiangsu Province (Grant No. BK20161390).

[1]L. Childress, R. Walsworth, and M. Lukin, Phys. Today **67**(10), 38 (2014).
[2]N. B. Manson and J. P. Harrison, Diamond Relat. Mater. **14**, 1705 (2005).
[3]L. Childress, M. V. G. Dutt, J. M. Taylor, A. S. Zibrov, F. Jelezko, J. Wrachtrup, P. R. Hemmer, and M. D. Lukin, Science **314**, 281 (2006).
[4]A. Gali, Phys. Rev. B **79**, 235210 (2009).
[5]R. Hanson, F. M. Mendoza, R. J. Epstein, and D. D. Awschalom, Phys. Rev. Lett. **97**, 087601 (2006).
[6]P. Neumann, R. Kolesov, B. Naydenov, J. Beck, F. Rempp, M. Steiner, V. Jacques, G. Balasubramanian, M. L. Markham, D. J. Twitchen, F. Jelezko, and J. Wrachtrup, Nat. Phys. **6**, 249 (2010).
[7]F. Dolde, H. Fedder, M. W. Doherty, T. Nobauer, F. Rempp, G. Balasubramanian, T. Wolf, F. Reinhard, L. C. L. Hollenberg, F. Jelezko, and J. Wrachtrup, Nat. Phys. **7**, 459 (2011).
[8]G. Balasubramanian, I. Y. Chan, R. Kolesov, M. Al-Hmoud, J. Tisler, C. Shin, C. Kim, A. Wojcik, P. R. Hemmer, A. Krueger, T. Hanke, A. Leitenstorfer, R. Bratschitsch, F. Jelezko, and J. Wrachtrup, Nature **455**, 648 (2008).
[9]J. R. Maze, P. L. Stanwix, J. S. Hodges, S. Hong, J. M. Taylor, P. Cappellaro, L. Jiang, M. V. G. Dutt, E. Togan, A. S. Zibrov, A. Yacoby, R. L. Walsworth, and M. D. Lukin, Nature **455**, 644 (2008).
[10]G. Kucsko, P. C. Maurer, N. Y. Yao, M. Kubo, H. J. Noh, P. K. Lo, H. Park, and M. D. Lukin, Nature **500**, 54 (2013).
[11]F. Grazioso, B. R. Patton, P. Delaney, M. L. Markham, D. J. Twitchen, and J. M. Smith, Appl. Phys. Lett. **103**, 101905 (2013).
[12]M. W. Doherty, N. B. Manson, P. Delaney, F. Jelezko, J. Wrachtrup, and L. C. L. Hollenberg, Phys. Rep. **528**, 1 (2013).
[13]B. T. Webber, M. C. Per, D. W. Drumm, L. C. L. Hollenberg, and S. P. Russo, Phys. Rev. B **85**, 014102 (2012).
[14]P. Deák, B. Aradi, M. Kaviani, T. Frauenheim, and A. Gali, Phys. Rev. B **89**, 075203 (2014).
[15]M. V. Hauf, B. Grotz, B. Naydenov, M. Dankerl, S. Pezzagna, J. Meijer, F. Jelezko, J. Wrachtrup, M. Stutzmann, F. Reinhard, and J. A. Garrido, Phys. Rev. B **83**, 081304 (2011).

[16]B. Grotz, M. V. Hauf, M. Dankerl, B. Naydenov, S. Pezzagna, J. Meijer, F. Jelezko, J. Wrachtrup, M. Stutzmann, F. Reinhard, and J. A. Garrido, Nat. Commun. **3**, 729 (2012).
[17]N. Aslam, G. Waldherr, P. Neumann, F. Jelezko, and J. Wrachtrup, New J. Phys. **15**, 013064 (2013).
[18]K. Beha, A. Batalov, N. B. Manson, R. Bratschitsch, and A. Leitenstorfer, Phys. Rev. Lett. **109**, 097404 (2012).
[19]G. Waldherr, J. Beck, M. Steiner, P. Neumann, A. Gali, T. Frauenheim, F. Jelezko, and J. Wrachtrup, Phys. Rev. Lett. **106**, 157601 (2011).
[20]P. Siyushev, H. Pinto, M. Voros, A. Gali, F. Jelezko, and J. Wrachtrup, Phys. Rev. Lett. **110**, 167402 (2013).
[21]Y. Doi, T. Makino, H. Kato, D. Takeuchi, M. Ogura, H. Okushi, H. Morishita, T. Tashima, S. Miwa, S. Yamasaki, P. Neumann, J. Wrachtrup, Y. Suzuki, and N. Mizuochi, Phys. Rev. X **4**, 011057 (2014).
[22]P. Olivero, F. Bosia, B. A. Fairchild, B. C. Gibson, A. D. Greentree, P. Spizzirri, and S. Prawer, New J. Phys. **15**, 043027 (2013).
[23]B. C. Gallheber, M. Fischer, O. Klein, and M. Schreck, Appl. Phys. Lett. **109**, 141907 (2016).
[24]D. J. Eaglesham and M. Cerullo, Phys. Rev. Lett. **64**, 1943 (1990).
[25]S.-H. Wei and A. Zunger, Phys. Rev. B **49**, 14337 (1994).
[26]D. Usachov, A. Fedorov, O. Vilkov, V. K. Adamchuk, L. V. Yashina, L. Bondarenko, A. A. Saranin, A. Grüneis, and D. V. Vyalikh, Phys. Rev. B **86**, 155151 (2012).
[27]J. Cheng, X. Yang, L. Sang, L. Guo, A. Hu, F. Xu, N. Tang, X. Wang, and B. Shen, Appl. Phys. Lett. **106**, 142106 (2015).
[28]E. R. MacQuarrie, T. A. Gosavi, N. R. Jungwirth, S. A. Bhave, and G. D. Fuchs, Phys. Rev. Lett. **111**, 227602 (2013).
[29]D. J. Shu, S. T. Ge, M. Wang, and N. B. Ming, Phys. Rev. Lett. **101**, 116102 (2008).
[30]Z. W. Wang, D. J. Shu, M. Wang, and N. B. Ming, Phys. Rev. B **82**, 165309 (2010).
[31]D. V. Potapenko, Z. Li, J. W. Kysar, and R. M. Osgood, Nano Lett. **14**, 6185 (2014).
[32]T. Karin, S. Dunham, and K.-M. Fu, Appl. Phys. Lett. **105**, 053106 (2014).
[33]M. W. Doherty, V. V. Struzhkin, D. A. Simpson, L. P. McGuinness, Y. Meng, A. Stacey, T. J. Karle, R. J. Hemley, N. B. Manson, L. C. L. Hollenberg, and S. Prawer, Phys. Rev. Lett. **112**, 047601 (2014).
[34]S. Bennett, N. Yao, J. Otterbach, P. Zoller, P. Rabl, and M. Lukin, Phys. Rev. Lett. **110**, 156402 (2013).
[35]J. Teissier, A. Barfuss, P. Appel, E. Neu, and P. Maletinsky, Phys. Rev. Lett. **113**, 020503 (2014).
[36]E. R. MacQuarrie, M. Otten, S. K. Gray, and G. D. Fuchs, Nat. Commun. **8**, 14358 (2017).
[37]P. E. Blöchl, Phys. Rev. B **50**, 17953 (1994).
[38]A. Gali, E. Janzén, P. Deák, G. Kresse, and E. Kaxiras, Phys. Rev. Lett. **103**, 186404 (2009).
[39]C. A. Klein, Mater. Res. Bull. **27**, 1407 (1992).
[40]R. H. Telling, C. J. Pickard, M. C. Payne, and J. E. Field, Phys. Rev. Lett. **84**, 5160 (2000).
[41]H. A. Jahn and E. Teller, Proc. R. Soc. London, Ser. A **161**, 220 (1937).
[42]H.-P. Komsa, T. T. Rantala, and A. Pasquarello, Phys. Rev. B **86**, 045112 (2012).
[43]C. Freysoldt, B. Grabowski, T. Hickel, J. Neugebauer, G. Kresse, A. Janotti, and C. G. Van de Walle, Rev. Mod. Phys. **86**, 253 (2014).
[44]G. Makov and M. C. Payne, Phys. Rev. B **51**, 4014 (1995).
[45]S. H. Wei, Comput. Mater. Sci. **30**, 337 (2004).
[46]W. J. Yin, J. Ma, S. H. Wei, M. M. Al-Jassim, and Y. Yan, Phys. Rev. B **86**, 045211 (2012).
[47]C. G. Van de Walle, J. Appl. Phys **95**, 3851 (2004).
[48]S. Lany and A. Zunger, Phys. Rev. B **78**, 235104 (2008).
[49]S. B. Zhang, J. Phys. Condens. Matter. **14**, R881 (2002).
[50]H. Pinto, R. Jones, D. W. Palmer, J. P. Goss, A. K. Tiwari, P. R. Briddon, N. G. Wright, A. B. Horsfall, M. J. Rayson, and S. Öberg, Phys. Rev. B **86**, 045313 (2012).
[51]P. Ágoston, K. Albe, R. M. Nieminen, and M. J. Puska, Phys. Rev. Lett. **103**, 245501 (2009).
[52]C. G. Van de Walle, S. Limpijumnong, and J. Neugebauer, Phys. Rev. B **63**, 245205 (2001).